3D SINGLE GAAS CO-AXIAL NANOWIRE SOLAR CELL FOR NANOPILLAR-ARRAY PHOTOVOLTAIC DEVICE

Khomdram Jolson Singh[1], Chelsea Leiphrakpam[1], Nongthombam Palbir Singh[1], N.Basanta Singh[1], Subir Kumar Sarkar[2]

[1]Dept. of Electronics and Communication Engineering, Manipur Institute of Technology ,Imphal-795004(India)
[2] Dept. of Electronics and Telecommunication Engineering, Jadavpur University ,Kolkata 700032(India)

ABSTRACT

Nanopillar array photovoltaics give unique advantages over today's planar thin films in the areas of optical properties and carrier collection, arising from their 3D geometry. The choice of the material system, however, is essential in order to gain the advantage of the large surface/interface area associated with nanopillars. Therefore, a well known Si and GaAs material are used in the design and studied in this nanowire application. This work calculates and analyses the performance of the coaxial GaAs nanowire and compared with that of Si nanowire using a semi-classical method. The current-voltage characteristics are investigated for both under dark and AM1.5G illumination. It is found that GaAs nanowire gives almost double efficiency with its counterpart Si nanowire. Their TCAD simulations can be validated reasonably with that of published experimental result.

KEYWORDS

Nanopillar-based photovoltaics, solar cells, nanowires (NWs).

1. INTRODUCTION

This Nanostructures are generally use as a new approach to reduce both cost and size with good efficiency in photovoltaics[1–9]. In different solar cell designs and materials such as Dye sensitized solar cells, polymerblend, ZnO, TiO_2 , these nanoparticles, nanorods and nanowires structures have been used to improve charge collection efficiency[4,5,6], to demonstrate carrier multiplication[7], and to enable low-temperature processing of photovoltaic devices[3–6]. Moreover, recent theoretical studies have indicated that coaxial nanowire structures could improve carrier collection and overall efficiency with respect to single-crystal bulk semiconductors of the same materials [8, 9]. However, solar cells based on hybrid nanoarchitectures have shown relatively low efficiencies and poor stabilities [1]

In the present work, we report the theoretical realization of p-type/intrinsic/ n-type (p-i-n) coaxial GaAs nanowire solar cells. This was further validated by comparing with experimental data of p-i-n coaxial Si nanowire reported in recent literatures. Under one solar equivalent (1-sun) illumination, the p-i-n GaAs nanowire elements yield an apparent energy conversion efficiency of up to 3.4 per cent, with stable and improved efficiencies achievable at high-flux illuminations. Furthermore, we have shown that interconnected GaAs nanowire photovoltaic elements to form

DOI:10.5121/ijcsa.2014.4309

nano-pillar array photovoltaic can serve as more efficient power sources. These coaxial GaAs nanowire photovoltaic elements provide a new nanoscale test bed for studies of photo induced energy/charge transport and artificial photosynthesis[10], and might find general usage as elements for powering ultra low power electronics[11] and diverse nanosystems[12,13] or nano-pillar array photovoltaic system.

We have focused on p-i-n coaxial GaAs nanowire structures (Fig.1) consisting of a p-type GaAs nanowire core capped with i- and n-type GaAs shells. An advantage of this core/shell architecture is that carrier separation takes place in the radial versus the longer axial direction, with a carrier collection distance smaller or comparable to the minority carrier diffusion length [8]. Hence, photogenerated carriers can reach the p-i-n junction with high efficiency without substantial bulk recombination. An additional consequence of this geometry is that material quality can be lower than in a traditional p-n junction device without causing large bulk recombination [1]. The highly conductive n-shell will reduce or eliminate potential drop along the shell, thereby enabling uniform radial carrier separation and collection when illuminated [8].

2. PHOTOVOLTAIC SIMULATION

2.1. Nanowire modeling

We simulate the device shown in Fig. 1 using ATLAS, a 2D/3D semiconductor device simulator [10]. Due to its symmetry, we simulate the device only in two dimensions and use the cylindrical coordinate system. The radius of the core p-type nanowire is 100 nm. The thicknesses of the i-layer and the n-type layer are 80 nm and 100 nm respectively. This gives us a nanowire with a diameter size of 360 nm. This diameter size is about the same as size of the nanowires in [2].

Fig. 1 Simulation scheme of a coaxial nanowire

The length of our nanowire, on the other hand, is set to be one micron which is smaller than the one in [2]. The reason for using a smaller nanowire length is to save computational time. The electrodes are placed so as to immitate the configuration shown in Fig. 1. The transport properties are calculated using the drift diffusion model. using such a semi-classical approach for the nanowire size considered in this work has been discussed in [11], [12]. In the calculation, we enabled the Shockley-Read-Hall recombination and concentration dependent mobility. We first solved the Poisson-Schrodinger equations self-consistently to see whether any quantum effect can be observed. But the results suggest that the quantum confinement effect is pretty small. Using an infinite potential well approximation, the first bound state is only about 0.01 meV above the conduction band, which supports the conclusion of the self-consistent calculation. The dark current-voltage characteristic was first obtained. The potential and the band energy of the coaxial nanowires were calculated self-consistently. After the dark properties were obtained, the nanowire was illuminated with AM 1.5 Global solar irradiance. The spectrum of this solar illumination is shown in Fig. 2. To perform this illumination we enabled the multi-spectral photogeneration in the simulator. The power of the solar spectrum was scaled by $1{:}5x10^{-3}$ to give a short circuit current in the pico Ampere range. The generation rate is calculated from

$$G = \eta_0 \frac{P\lambda}{hc} \alpha e^{-\alpha y}$$

with G being the photogeneration rate, P the cumulative effects of reflections, transmissions, and loss due to absorption over the ray path, y the relative distance for the given ray, *h* the Planck's constant, λ the wavelength, *c* the speed of light and α the absorption coefficient calculated for each set of (n, k) value. Absorption coefficient is defined as the number of photon absorbed for a particular wavelength (λ) incident on it. It is a property of material that cannot be modified. It is also related to the extinction coefficient, *k*, by the following formula:

$$\alpha(\lambda) = \frac{4\pi k}{\lambda} 10^7 \, cm^{-1}$$

where λ in nm.

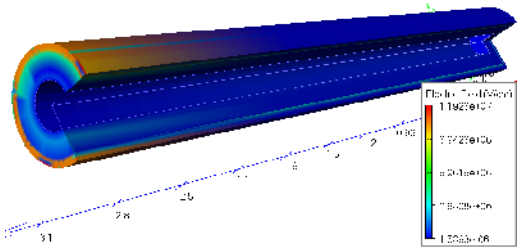

Fig. 3 Electric Field Profile

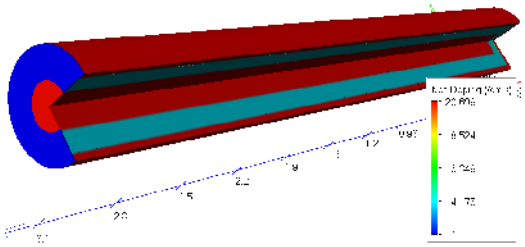

Fig. 5 Net Doping Profile

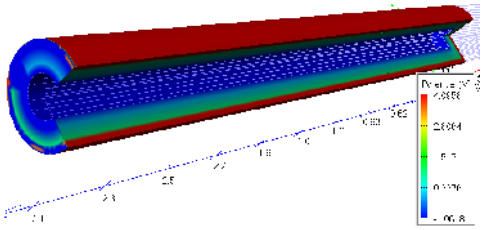

Fig. 4 Potential Generated Profile

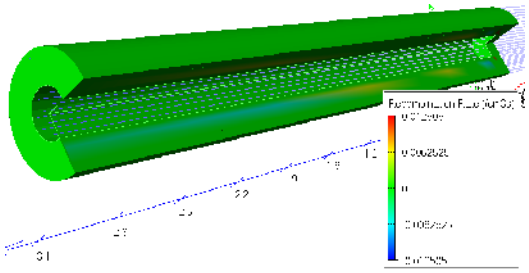

Fig. 6 Recombination Rate Profile

Fig.3-6 represent the different profile generated from the model illuminated with AM 1.5G. The legend within the figure defines the solar cell's photogeneration rates. These are expressed using the log of the electron-hole pair generation rates that correspond to the color-coded display. For example the highest numerical value (e.g., 23) corresponds to the color-coded horizontal layer that is generating10^{23} electron-hole pairs per cm^3. Here, most of the higher photo generation rates are observed in the upper solar cell layers because a significant majority of the photon energy is absorbed here prior to reaching the remaining body (e.g., the yellow region) of the simulated device.

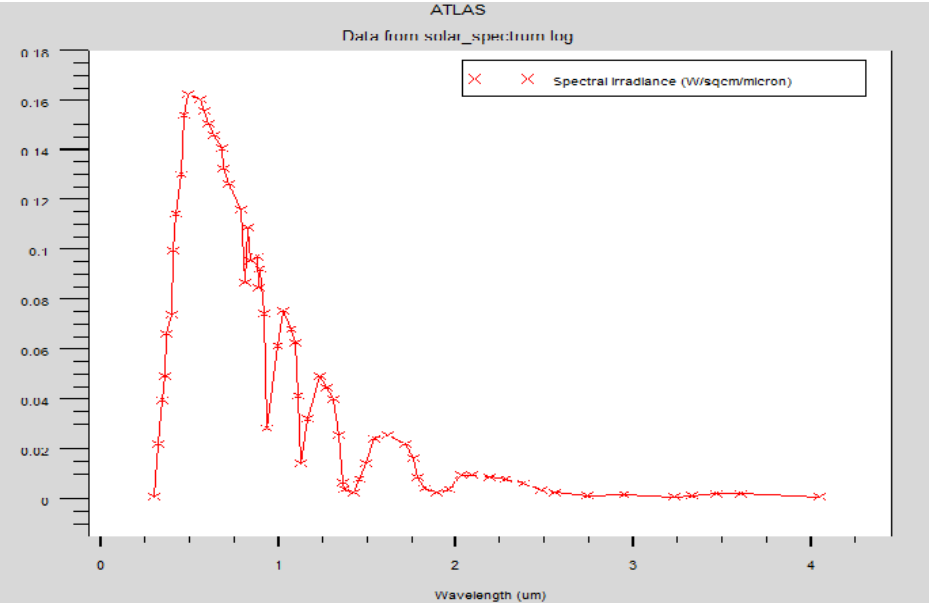

Fig. 2 Solar spectrum air mass 1.5 global (AM 1.5 G) irradiance.

2.2. TCAD Simulation

Table 1 Important parameters used in the simulation[10]

Material	GaAs
Band gap Eg[eV] @300^{o}K	1.42
Lattice constant α [Å]	5.65
Permittivity es/eo	13.1
Affinity [eV]	4.07
Heavy e– effective mass [me*/m0]	0.063
Heavy h+ effective mass [mh*/m0]	0.5
e– mobility MUN [cm^2/V×s]	8800
h+ mobility MUP [cm^2/V×s]	400
e–density of states NC [cm^{-3}]	4.7E+17
h+density of states NV [cm^{-3}]	7.0E+18
ni (per cc)	2.1E+06
Vsatn (cm/s)	7.7E+06
Vsatp (cm/s)	7.7E+06

To work as a nanoscale power supplies, the output power must be higher than a few nanoWatt. In order to increase the power, the light intensity should be larger, or several nanowires should be used together.Next, we plot the photogeneration rate along the radial direction. We expect that the curve is higher than the exponential behaviour of intensity decay in a bulk material. The reason is that in this simulation we illuminate the nanowire all around. And hence, there is illumination from other sides of the nanowire, which results in a higher absorption by the nanowire. In reality, however, the illumination usually only occurs from only one direction rather than all around. In this case, a three

dimension simulation must be performed to study the photogeneration rate inside the nanowire.

3. RESULT AND DISCUSSION

The The core/shell silicon nanowire diodes were further characterized by analysing data recorded with and without the i-layer as a function of temperature. Fits to ln(I)–V data recorded in forward bias from p-i-n and p-n coaxial structures are linear, and yield diode ideality factors N of 1.96 and 4.52, respectively. The N-values show that introduction of the i-layer yields much better quality diodes. Reverse bias measurements from p-i-n and p-n diodes also show markedly different behaviour: the p-i-n diode breaks down at much larger reverse-bias voltage (approximately 27 V) than the p-n diode (approximately 21 V) for all temperatures studied. In addition, the reverse-bias breakdown voltage of the p-n diode increases with decreasing temperature, which is consistent with a Zener (tunneling) breakdown mechanism, whereas the breakdown voltage of the p-i-n structures exhibits little temperature dependence, suggesting contributions from tunneling and avalanche mechanisms[11]

Overall, these results indicate that tunneling or leakage currents are more significant in the p-n diode[12], and that the diode quality factor and breakdown behavior are readily controlled during nanowire growth by the introduction of the i-layer as in planar structures[13,14].

Likewise, the photovoltaic properties of the p-i-n coaxial GaAs nanowire diodes were characterized under air mass 1.5 global (AM 1.5G) illumination. I–V data recorded from one of the better devices (Fig. 10) yields an open-circuit voltage Voc of 0.56 V, a short-circuit current Isc of 0.258 nA and a fill factor Ffill of 55.0%. The maximum power output Efficiency for the GaAs nanowire device at 1-sun is 16.9%.

Measurements of Isc as a function of the p-i-n coaxial GaAs nanowire length show linear scaling with values of 1 nA silicon nanowire–1 readily achieved for lengths of 10 mm (1-sun), whereas Voc is essentially independent of length. The linear scaling of Isc with silicon nanowire length suggests that photogenerated carriers are collected uniformly along the length of these radial nanostructures, and that scattering of light by the metal contacts does not make a major contribution to the observed photocurrent.

Table 2 Output parameters obtained from the simulated model

P-i-N material	**Suns**	**Jsc (mA/cm^2)**	**Vm (V)**	**Im (A)**	**Eff %**
GaAs	1	2.53296e-011	0.56	2.52273e-011	16.6
GaAs	10	2.56607e-011	0.56	2.55204e-011	16.8
GaAs	100	2.58634e-011	0.56	2.57486e-011	16.9
Si	100	1.75109e-011	0.48	1.63699e-011	9.2

The apparent photovoltaic efficiency of this device is 16.9 % (upper bound) and 16.6% (lower bound), but might be improved through increased understanding of absorption and better coupling of light into the devices, for example, by vertical integration [8] or multilayer stacking. Isc and Voc depend linearly and logarithmically, respectively, on the light intensity incident on the chip, consistent with systematic increase in photogenerated carriers[14]. We note that the apparent

efficiency is substantially higher at multiple-sun illumination . Although this apparent efficiency enhancement is larger than that in a planar silicon solar cell [14], it is consistent with the larger ideality factor (N) and lower 1-sun Voc of the nanowire devices [19]. Analysis of a plot of ln(Isc) versus Voc (Fig. 10) yields values of the diode ideality factor and saturation current of N51.86 and I052.72 pA, respectively. These values are similar to those extrapolated from the dark measurements (N51.96, I053.24 pA), and thus demonstrate good consistency in the behaviour and analysis of these core/shell GaAs nanowire diode devices.

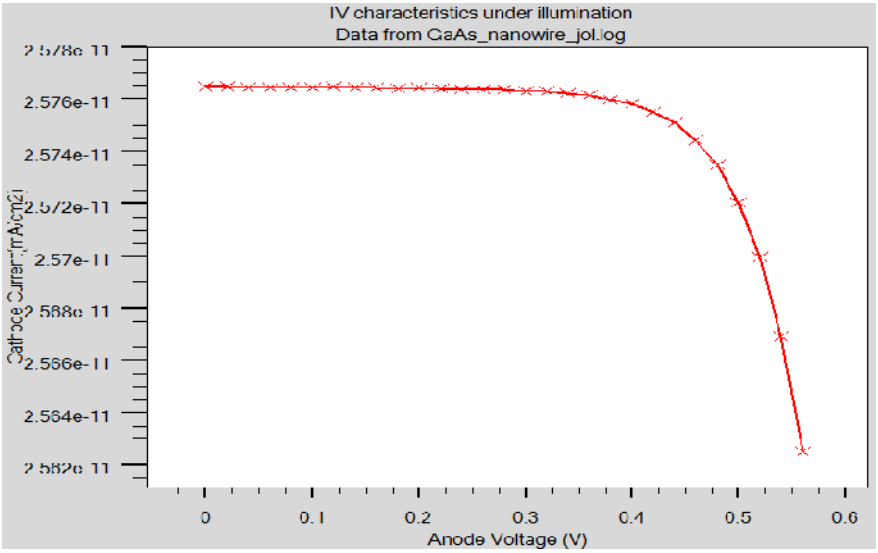

Fig. 10 I-V characteristic under AM1.5G illumination.

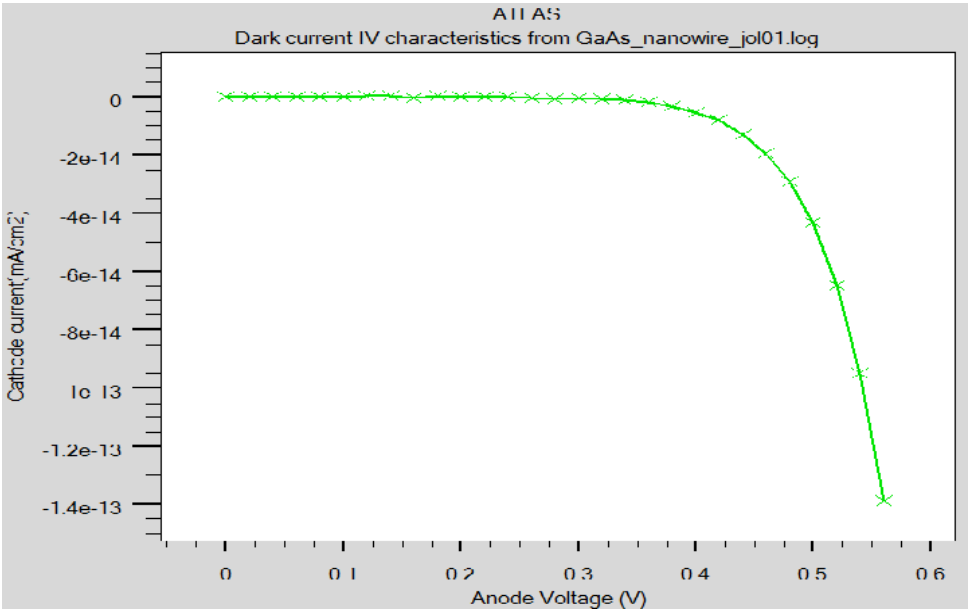

Fig.11 Dark current I-V characteristic

I–V data analysis. The saturation current, I_0, together with the diode ideality factor N was extrapolated from the dark I–V curve using the ideal diode equation:

$$\ln(I) = \frac{q}{NkT}V + \ln(I_0)$$

where q is the electronic charge and k is the Boltzmann constant. The average's ideality factor values obtained from the analysis of p-i-n and p-n coaxial GaAs nanowire were 3.33 and 5.82, respectively. Under illumination, the ideal diode equation can be expressed in terms of Isc and Voc as:

$$\ln(I_{sc}) = \frac{q}{NkT}V_{oc} + \ln(I_0)$$

where fits to ln(Isc) versus Voc are used to determine Nand I_0 from the slope and intercept, respectively.

Our core/shell GaAs nanowire results can be compared to nanocrystal-based [4] and nanorod-based [5,6] photovoltaic devices. The best silicon nanowire device exhibits large apparent short-circuit current densities—23.9mAcm^{-2} (upper bound) and 16.0mAcm^{-2} (lower bound)—with upper limits that are comparable to the 24.4mAcm2 value for the best thin film nanocrystalline silicon solar cell[24], and substantially better than values reported for CdSe nanorod/poly-3-hexathiophene4 and dye-sensitized ZnO nanorod [5,6] solar cells. The Voc value, 0.260 V, is 2–2.8 times lower than reported in these previous studies [4–6],[24] and represents an area that should be addressed in future studies. However, the overall apparent efficiency of the p-i-n coaxial silicon nanowire photovoltaic elements—3.4% (upper bound) and 2.3% (lower bound)—exceeds reported nanorod/polymer and nanorod/dye systems[4–6], and could be increased substantially with improvements in Voc by means of, for example, surface passivation. In addition, increasing the illumination intensity can yield stable improvements in the apparent efficiency of our p-i-n coaxial silicon nanowire photovoltaic elements in contrast to other nanostructured solar cells, which often exhibit degradation [4–6].

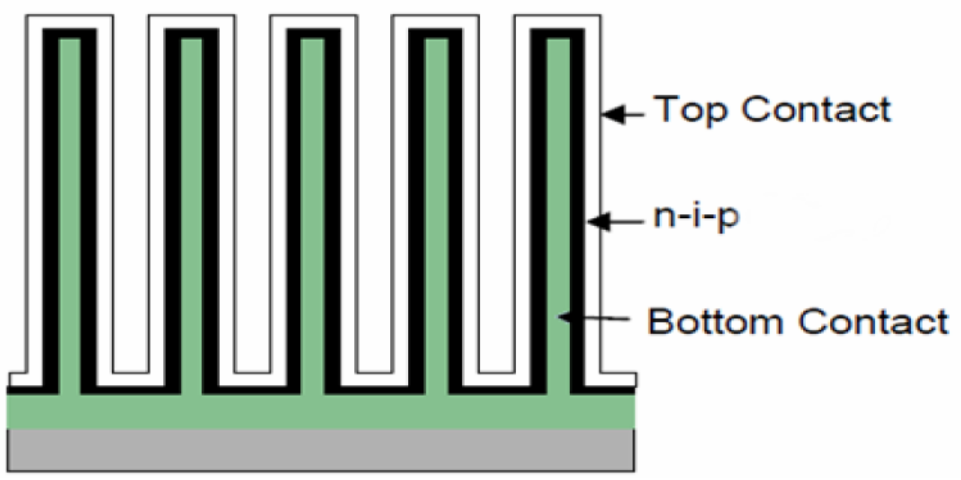

Fig.7 Nanopillar- array PV system

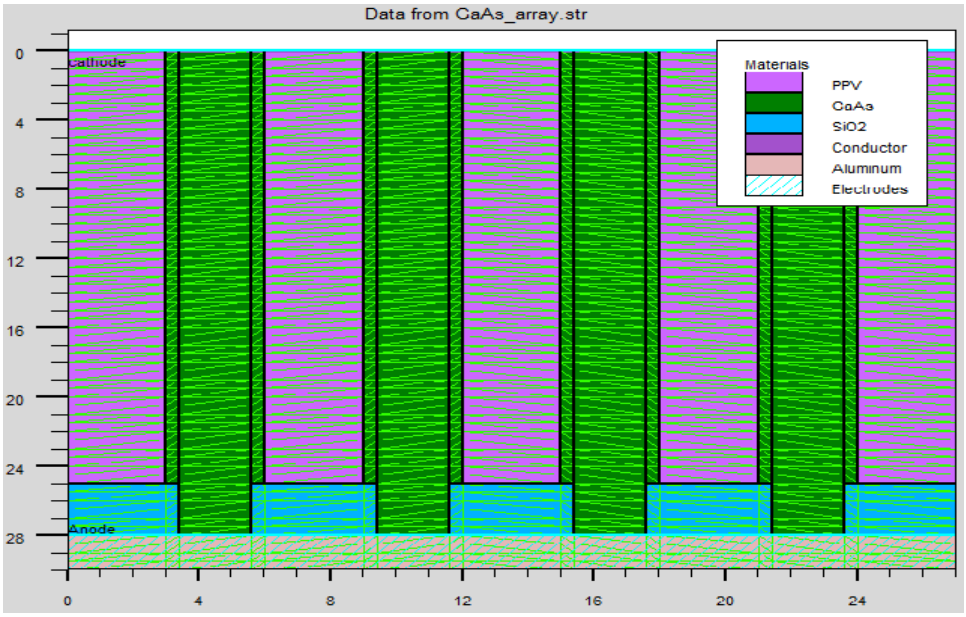

Fig.8 Nanopillar- array PV system simulated in TCAD

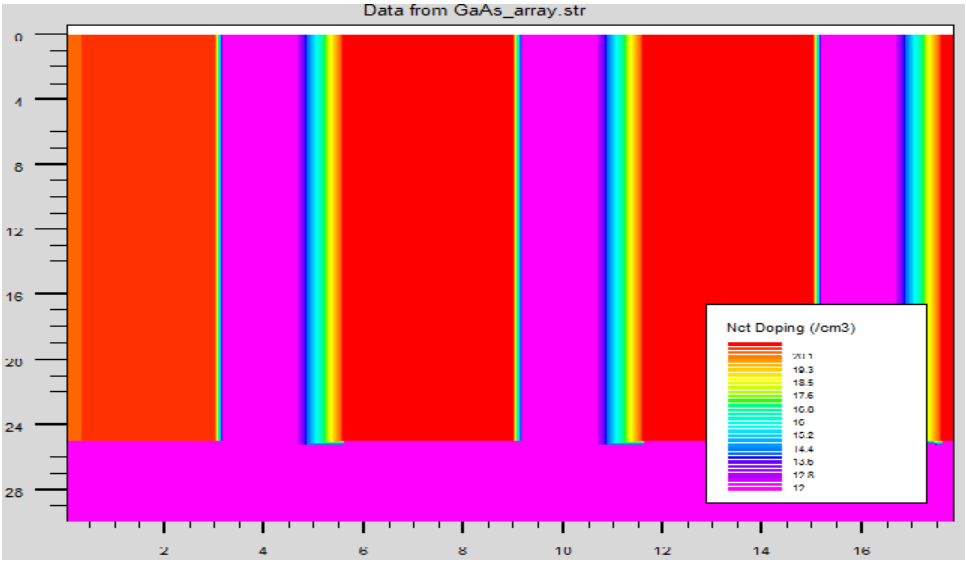

Fig. 9 Nanopillar- array net dping profile

Last, the core/shell GaAs nanowire photovoltaic devices were interconnected in series and in parallel to demonstrate scaling of the output characteristics and to drive larger loads. I–V data recorded from three illuminated GaAs nanowire elements (Fig. 7-9) show several important features. First, the individual elements exhibit very similar behaviour, highlighting the good reproducibility of our core/shell nanowire devices. Second, interconnection of the three elements forming nanopillar array in series and parallel yields Voc and Isc values, respectively, that are approximately the sum of three, as expected. Moreover, we observed that GaAs nanowire gives almost double efficiency with its counterpart Si nanowire even under 100 suns illumination and the detailed comparison is given in Table 2.

4. CONCLUSIONS

This work simulate and model both the coaxial silicon and GaAs nanowire photovoltaic devices using the standard TCAD tool. The 3D structure gives more insight of the model. And it is observed that GaAs nanowire perform much better than Si nanowire. These co-axial nanowire can further connected together to form nanopillar array PV system to generate more power.The methodology used and accuracy of the 3D model can be helpful for further research and application in this nano PV regime. It was also shown by other researchers that such a device is able to power up nanoelectronics devices that require power in the range of nanoWatt.

ACKNOWLEDGEMENTS

Sincere gratitude to my supervisor Pof S.K Sarkar and Associate Prof. N.Basanta Singh. And also thanks to the Spintronics/Low Power VLSI Device Lab, ETCE Dept. Jadavpur University for providing the SILVACO TCAD Tools software.

REFERENCES

[1] Lewis, N. S. Toward cost-effective solar energy use. Science 315, 798– 801 (2007).
[2] Lewis, N. S. & Crabtree, G. (eds) Basic Research Needs for Solar Energy Utilization.(Report of the Basic Energy Sciences Workshop on Solar Energy Utilization, US Department of Energy, Washington DC, 2005); ,http://www.er.doe.gov/bes/reports/abstracts.html#SEU. (18–21 April, 2005).
[3] Gratzel, M. Photoelectrochemical cells. Nature 414, 338–344 (2001).
[4] Huynh, W. U., Dittmer, J. J. & Alivisatos, A. P. Hybrid nanorod-polymer solar cells. Science 295, 2425–2427 (2002).
[5] Law, M., Greene, L. E., Johnson, J. C., Saykally, R. & Yang, P. Nanowire dyesensitized solar cells. Nature Mater. 4, 455–459 (2005).
[6] Baxter, J. B. & Aydil, E. S. Nanowire-based dye-sensitized solar cells. Appl. Phys. Lett. 86, 053114 (2005).
[7] Luque, A., Marti, A. & Nozik, A. J. Solar cells based on quantum dots: multiple exciton generation and intermediate bands. MRS Bull. 32, 236–241 (2007).
[8] Kayes, B. M., Atwater, H. A. & Lewis, N. S. Comparison of the device physics principles of planar and radial p-n junction nanorod solar cells. J. Appl. Phys. 97, 114302 (2005).
[9] Zhang, Y., Wang, L. W. & Mascarenhas, A. Quantum coaxial cables. Nano Lett. 7, 1264–1269 (2007).
[10] Process and Device, 2D and 3D Physics-based Simulation, SILVACO International www.silvaco.com.
[11] Hayden, O., Agarwal, R. & Lieber, C. M. Nanoscale avalanche photodiodes for highly sensitive and spatially resolved photon detection. Nature Mater. 5, 352–356 (2006).
[12] Karpov, V. G., Cooray, M. L. C. & Shvydka, D. Physics of ultrathin photovoltaics. Appl. Phys. Lett. 89, 163518 (2006).
[13] Shah, A. V. et al. Thin-film silicon solar cell technology. Prog. Photovolt. Res. Appl. 12, 113–142 (2004).
[14] Luque, A. & Hegedus, S. Handbook of Photovoltaic Science and Engineering (Wiley, Chichester, 2003).

Authors

Khomdram Jolson Singh is Assistant Prof.(ECE Dept.) MIT Imphal, Manipur University. (India).

Chelsea Leiphrakpam is a student of ECE Dept, Manipur Institute of Technology, Imphal (India).

Nongthombam Palbir Singh is a student of.ECE Dept., MIT Imphal, Manipur University. (India).

Nameirakpam Basanta Singh is Associate Professor MIT Imphal, Manipur University, (India).*Member, IEEE*

Subir Kumar Sarkar is Professor (ETCE Dept.), Jadavpur University, (India). *Senior Member, IEEE*

.